



**HAL**  
open science

## Controlled Bioactivity in Zn-doped sol-gel derived SiO<sub>2</sub>-CaO bioactive glasses

Laurence Courthéoux, Jonathan Lao, Jean-Marie Nedelec, Edouard Jallot

► **To cite this version:**

Laurence Courthéoux, Jonathan Lao, Jean-Marie Nedelec, Edouard Jallot. Controlled Bioactivity in Zn-doped sol-gel derived SiO<sub>2</sub>-CaO bioactive glasses. *Journal of Physical Chemistry C*, 2008, 112 (35), pp.13663-13667. 10.1021/jp8044498 . hal-00360357

**HAL Id: hal-00360357**

**<https://hal.science/hal-00360357v1>**

Submitted on 11 Feb 2009

**HAL** is a multi-disciplinary open access archive for the deposit and dissemination of scientific research documents, whether they are published or not. The documents may come from teaching and research institutions in France or abroad, or from public or private research centers.

L'archive ouverte pluridisciplinaire **HAL**, est destinée au dépôt et à la diffusion de documents scientifiques de niveau recherche, publiés ou non, émanant des établissements d'enseignement et de recherche français ou étrangers, des laboratoires publics ou privés.

# Controlled Bioactivity in Zn-doped sol-gel derived SiO<sub>2</sub>-CaO bioactive glasses

L. Courthéoux<sup>1,2</sup>, J. Lao<sup>1</sup>, J.-M. Nedelec<sup>3</sup>, E. Jallot<sup>1</sup>.

<sup>1</sup> *Laboratoire de Physique Corpusculaire de Clermont-Ferrand CNRS/IN2P3 UMR 6533*

*Université Blaise Pascal – 24 avenue des Landais, 63177 Aubière Cedex, France.*

<sup>2</sup> *Institut Charles Gerhardt Montpellier UMR 5253 CNRS-UM2-ENSCM-UM1*

*Place E. Bataillon, cc 1503, 34095 Montpellier Cedex 5, France.*

<sup>3</sup> *Laboratoire des Matériaux Inorganiques CNRS UMR 6002*

*Université Blaise Pascal & ENSCCF – 24 avenue des Landais, 63177 Aubière Cedex,  
France.*

## ***Abstract***

Sol-gel derived glasses based on SiO<sub>2</sub>-CaO were studied with and without Zn as doping element. Investigations of their *in vitro* bioactivity were performed by soaking the glass powders in biological fluids for time periods up to 4 days. The surface reactions were characterized at the micrometer scale and with a high level of efficiency for both major and trace elements by using Particle Induced X-ray Emission (PIXE) associated to Rutherford Backscattering Spectroscopy (RBS). The evolution of the biological medium composition was followed by ICP-AES analyses. If the bioactivity of binary SiO<sub>2</sub>-CaO glasses is already known, this study shows the improvement of the early step of the bioactive process by using zinc as a doping element. Indeed, zinc improves the specific surface area and then the number of sites for the nucleation of calcium phosphate precipitates. In addition, Zn-doping slows the

---

<sup>1</sup> Corresponding author: jallot@clermont.in2p3.fr

glass dissolution and enhances the calcium phosphate layer growth at the surface of the ZnO-SiO<sub>2</sub>-CaO glass which is a prerequisite for bioactive glasses to bond to living bone.

**Keywords:** sol-gel glasses; bioactivity; Zn doped glasses; PIXE-RBS; biomaterials.

## ***Introduction***

Since about forty years, bioactive glasses based on silica have been extensively studied for bone repair or replacement.<sup>1,2</sup> Indeed, in contact with living tissues, bioactive materials allow the formation at their surface of a Ca-P rich layer similar to the bone mineral phase and then an effective bonding with the bone. Glass composition and textural properties such as high surface area and porosity are key factors for the bioactive process. In a few words, the bioactive process consists of well known series of physico-chemical reactions between the glass and the biological solution leading to the formation of a hydroxyapatite layer at the surface of the glass.<sup>3,4</sup> The first step of the bioactive process is a rapid cations exchange between the glass and the solution, followed by silica dissolution and formation of silanols groups at the glass/solution interface. Then polycondensation reactions of surface silanols generate a silica-rich layer which provides favorable sites for the formation of Ca-P layer. The calcium phosphates progressively crystallize, by incorporation of anions from the solution, into a biologically reactive hydroxycarbonate apatite equivalent to the mineral phase of bone.<sup>5,6</sup> It can be noticed that the formation of stable apatite is closely dependent on the textural properties of the materials but also on its composition.<sup>7</sup> That is why the many advantages of sol-gel glasses over melt derived analogues have favored their development as bioactive materials.<sup>8,9,10</sup> In fact, the sol-gel procedure leads to very homogeneous and high specific surface area materials and its versatility allows reaching a large range of composition.

Among bioactive sol-gel materials, very simple compositions, as for example SiO<sub>2</sub>-CaO glasses, have shown interesting bioactive properties.<sup>11,12</sup> Moreover, the study of the Ca-

P layer growth process is easier in such binary system, since the phosphate ions are only coming from the solution by comparison with the SiO<sub>2</sub>-CaO-P<sub>2</sub>O<sub>5</sub> ternary system. To improve the bioactivity of such glasses, additives can be easily introduced during the sol-gel synthesis. The doping elements are generally chosen among human body trace elements and for their biological activity. Several authors have reported the influence of silver to improve the formation of hydroxyapatite<sup>13</sup> or for antibacterial properties.<sup>14,15</sup> Besides silver, other doping elements, like Mg or Sr for example, have been studied to promote the bioactivity of glasses.<sup>16,17,18</sup> Zinc is another essential trace element in human body which has shown a stimulatory effect on bone formation.<sup>19,20</sup> Namely very few paper deals with Zn influence on the bioactive process in sol-gel glasses and there is still a lack of quantitative information regarding the physico-chemical reactions occurring at the interface of such glasses.

The aim of this paper is, thus, to study the influence of Zn as a doping element on the bioactivity of SiO<sub>2</sub>-CaO glasses. For this purpose, Zn doped SiO<sub>2</sub>-CaO bioactive glasses were elaborated using the sol-gel method and tested by immersion in biological fluids for different time periods. Evolution of elemental distributions at the biomaterial/biological fluids interface were highlighted with the Particle Induced X-ray Emission (PIXE) technique associated to Rutherford Backscattering Spectroscopy (RBS). The evolution of the biological fluids composition was followed by ICP-AES (Inductively Coupled Plasma-Atomic Emission Spectroscopy) analyses.

## ***Materials & methods***

### *Preparation of the bioactive glass samples*

The bioactive powder containing 75wt% SiO<sub>2</sub>-25wt% CaO was chosen as reference in order to study the influence of doping for different ZnO content: 1 wt% ZnO for Zn1 and 5 wt% ZnO for Zn5. The Zn-doped bioactive glasses based on silica were prepared by a classical sol-gel method as follows. Tetraethylorthosilicate (TEOS; Si(OC<sub>2</sub>H<sub>5</sub>)<sub>4</sub>), calcium

nitrate ( $\text{Ca}(\text{NO}_3)_2, 4\text{H}_2\text{O}$ ) and zinc nitrate ( $\text{Zn}(\text{NO}_3)_2, 6 \text{H}_2\text{O}$ ) were mixed in ethanol in presence of water and hydrochloric acid as catalyst. The sol was then transferred to an oven at  $60^\circ\text{C}$  during four hours followed by a drying at  $125^\circ\text{C}$  for 24 hours for gelification and aging. The xerogel was finally grinded to powder and calcined at  $700^\circ\text{C}$  for 24 hours.

### *Characterizations*

The specific surface area of the samples was calculated with the BET method during nitrogen adsorption-desorption using a Quantachrome Porosimeter Autosorb-1. Prior to the experiments, the samples were outgassed at  $120^\circ\text{C}$  for 12h to remove physically adsorbed molecules such as moisture. The surface structure has also been observed with a ZEISS Supra 55VP scanning electron microscope. Inductively Coupled Plasma-Atomic Emission Spectroscopy (ICP-AES) was used to determine the chemical composition of the bioactive powder and to analyze the biological fluids during interactions with bioactive glasses.

### *In vitro assays*

The interactions between the glasses and a biological medium have been carried out at  $37^\circ\text{C}$  for 1h, 6h, 1, 2, 3 and 4 days by immersing about 10 mg of powder in a standard Dulbecco's Modified Eagle Medium (DMEM), which composition is almost equal to human plasma. The specific surface area to DMEM volume ratio was fixed at  $500 \text{ cm}^{-1}$ . These *in vitro* assays were conducted under static conditions: biological fluids were not renewed and therefore contained only limited amount of P and Ca. Namely, this is a good approach for further development and to compare different doping elements and compositions. After interaction, the samples were removed from the fluid, air dried and embedded in resin (AGAR). Before characterization, the glass particles were cut into thin sections of 1 micrometer nominal thickness using a Leica EM UC6 Ultramicrotome, and laid out on 50 mesh copper grids. The grids were then placed on a Mylar film with a middle hole of 3 mm.

The analyses of the biomaterial/biological fluid interface were carried out using nuclear microprobes at the CENBG (Centre d'Études Nucléaires de Bordeaux-Gradignan,

France). The device provides a micro-beam line employed for ion beam analytical measurements at the microscopic level. Particle Induced X-ray Emission (PIXE) coupled with Rutherford Backscattering Spectroscopy (RBS) were used to get chemical mapping at the glass/biological fluid interface both for major components and trace elements.<sup>21</sup> For PIXE-RBS analyses, we chose proton scanning micro-beam of 3 MeV energy and 50 pA in intensity. Such settings resulted in higher ionization cross-sections and an increased sensitivity for the micro-analysis. The beam diameter was 1  $\mu\text{m}$ . An 80 mm<sup>2</sup> Si(Li) detector was used for X-ray detection, orientated at 135° with respect to the incident beam axis and equipped with a beryllium window 12  $\mu\text{m}$  thick. An Al-filter with a tiny 2 mm hole drilled at its centre (“funny filter”) was systematically placed in front of the Si(Li) detector; the funny filter allows the detection of heavy trace elements ( $Z \geq 25$ ) whereas it avoids the saturation of the detector by major light ( $Z \leq 20$ ) elements X-rays, since those latter are only detected through the small aperture. PIXE spectra were treated with the software package GUPIX. Relating to RBS, a silicon particle detector was placed at 135° from the incident beam axis and allowed the determination of the number of protons that interacted with the sample. Data were treated with the SIMNRA code. This methodology finally allowed quantifying major and trace elements concentrations at the micrometer scale.

## ***Results and discussion***

### *Bioactive glass characterization*

The experimental composition of each sample determined by ICP-AES analysis and their specific surface area are reported in Table 1. Thanks to the sol-gel synthesis, the final concentrations are very close to the nominal values and all the component are homogeneously distributed, as shown in the elemental maps of the 5% ZnO doped glass before immersion in biological fluids (Figure 1). All samples display a porous structure with significantly larger

specific surface area for Zn doped glasses. The SEM images (Figure 2) reveal a homogeneous porosity in the range of 50 to 100 nm for low Zn content whereas higher doping leads to larger pore size distribution, between 50 and 400 nm. This can be due to a modification of the glass network because of the insertion of Zn atoms in the SiO<sub>2</sub>-CaO structure by Ca substitution. Zn-doping also induces an increase in the specific surface area. A high surface area can be very attractive for further interaction with biological medium by providing more nucleation sites for the formation of phosphocalcic precipitates.

#### *In vitro tests for Zn doped and undoped SiO<sub>2</sub>-CaO glasses*

PIXE-RBS multi-elemental maps of the surface of the glasses were recorded for each immersion time in DMEM: they provide quantitative and qualitative information about major and trace elements at the interface between the glasses and biological fluids. The observed distributions correspond to the intensity of X-rays locally emitted by the sample under proton irradiation. Each elemental map was divided in various regions of interest depending on the distribution of chemical elements in order to determine the elemental concentrations. The values calculated correspond to the mean of concentrations determined in several zones of interest. These regions of interest were defined over various samples in order to be ensured of measurements reproducibility.

Briefly, physico-chemical interactions between glasses and biological fluids induce two concomitant mechanisms: the dissolution of the glass silicate network, and the rapid formation of a surface layer at the material periphery. Concerning the *in vitro* behaviour of the undoped sample, all the results have been published in detail in a previous paper<sup>21</sup>. For the undoped sample, within 15 minutes, the incorporation of phosphorus coming from the biological medium and of Ca ions coming both from the glass matrix and DMEM, leads to the formation of a calcium phosphate enriched layer at the grains periphery. However multielemental maps have shown that the newly formed calcium phosphate layer is unstable

and that it is quickly dissolved by biological fluids. After 2 days soaking, the calcium phosphate layer has been almost completely dissolved. These results suggest that the periphery of the undoped glass consists of amorphous calcium phosphates which composition significantly differs from that of hydroxyapatite (HA). The Si-rich core of the particle is finally the only region remaining since it is more resistant to dissolution. Indeed, after four days, the periphery of the SiO<sub>2</sub>-CaO glass is composed of 42.3% Si and only 3.8% Ca without any phosphorus.

The addition of zinc as doping element delays the breakdown of the glass silicate network from biological fluids. In fact, although the incorporation of phosphorus from the biological medium at the surface of the glass occurs during the first hours, the Ca diffusion from the core of the material to its periphery begins later on. Recent works investigating the structure of Zn-doped phosphosilicate glasses<sup>22</sup> may provide us with an explanation for this: it was found that Zn adopts a tetrahedral coordination in the glassy network and copolymerizes with [SiO<sub>4</sub>] tetrahedra. That results in an overall complexation of the glass network that finally leads to an increase of its chemical durability.

After one day of interaction, the Ca-P rich peripheral layer is clearly noticeable for low Zn content (Figure 3), surrounding the core of the material from which Ca has migrated. Higher doping concentration requires higher delay for Ca to migrate from the inner regions of the material to the periphery (Figure 4). After three days, all Zn-doped samples have formed a Ca-P rich peripheral layer. At that time the core of the grains is principally constituted of silicon and zinc oxides (Figure 5). The corresponding compositions for the glasses periphery are reported in Table 2. . Our results demonstrate that the higher the Zn content, the higher the calcium phosphates amount in the peripheral layer. After three days, the surface layer of Zn5 sample consists of 24.5% of Ca, 5.5% of P and only 19.7% of Si. By comparison, the undoped sample displays silicon rich grains (42.3%) with only a small amount of calcium (3.8%) and without any phosphorus. An essential observation is that the Ca-P peripheral layer



is not dissolved after a few days of interaction for Zn-doped glasses, contrary to what was observed for the undoped glass. It is an important indication on the formation of a HA-like layer: indeed HA is the most stable and least soluble of all calcium phosphates<sup>23</sup>.

To confirm these observations, we have calculated the Ca/P atomic ratio at the glass/biological fluids interface by creating thin regions of measurement 1  $\mu\text{m}$  wide at the material surface. Results are shown in Figure 6. For the undoped sample, the Ca/P atomic ratio firstly decreases but after 6h the Ca-P surface layer is quickly dissolved: calcium and especially phosphate ions are progressively leached into the biological medium. This phenomenon induces a high increase in the Ca/P atomic ratio at the surface of the undoped sample. For Zn doped samples, the Ca/P atomic ratio continuously decrease, corresponding to the Ca-P layer formation and growth. The ratio then stabilizes between 1.2 and 2.5, close to the theoretical hydroxyapatite ratio: 1.67. Thus there is evidence that the initially amorphous phosphocalcic layer is progressively transformed into a more stable apatite layer.

Physico-chemical reactions between the biological fluids and the bioactive glass powders have also been monitored by measuring the DMEM composition as a function of interaction time. Figure 7 shows that Si, Ca and Zn concentrations in biological fluids increase during the first interaction delays, due to their dissolution from the glass. Logically, the amount of Zn dissolved increases with its concentration in the glass. It can be noticed that the Zn-doped samples exhibit no or low Ca precipitation coming from the biological fluids but after four days of interaction, they lead to larger calcium release, despite a lower CaO content. At the same time, a decrease in P concentration in solution is observed, due to the Ca-P layer formation. The stabilization of Ca and Si concentrations in the solution is reached after one day; concerning P, the equilibrium is reached after two days for the undoped sample and for Zn1. For Zn5, the P concentration still decreases after three days. Higher zinc content involves the incorporation of more phosphorus atoms within the surface layer. Nevertheless,

longer interaction time should be used for 5% ZnO sample to be ensured of the system equilibrium.

To summarize, doping with zinc allows the early precipitation of phosphate ions from the biological fluids at the glass surface, as evidenced by Figure 3 and 6. Zn-doping also delays the glass dissolution and slows the growth of the calcium phosphate layer. This facilitates the gradual crystallization of stable HA and would therefore provide a better bone bonding interface *in vivo*. But the most attracting characteristics of Zn-doped glasses may be their ability to release physiological concentrations of Zn into the surrounding fluids. In fact the stimulating effect of Zn doped bioactive glasses have already been shown with CaO-P<sub>2</sub>O<sub>5</sub>-SiO<sub>2</sub> samples for cell differentiation<sup>24</sup> and alkaline phosphatase production.<sup>19</sup> Our study shows that Zn -doping modifies the kinetics of the early first steps of the bioactive process, even for P<sub>2</sub>O<sub>5</sub>-free glasses.

## ***Conclusion***

The Zn doping effect can be resumed in two parts: a textural effect and bioactive properties. By improving the specific surface area of the glass, more nucleation sites for apatite formation are available. In addition, Zn-doping slows the glass dissolution and improves the phosphorus incorporation. The results of our study highlight the major role of Zn as doping element to enhance the calcium phosphate surface layer formation and growth, which is a prerequisite for bioactive glasses to bond to living bone.. It is important to notice that the Ca-P rich layer grows up in an acellular environment and therefore its spontaneous formation was only due to the ZnO-SiO<sub>2</sub>-CaO bioactive properties. Further experiments with different glass compositions and in a cellular medium could give more informations concerning the specific role of Zn ions. One of our future prospects is therefore to control the

dissolution of the material along with the release of critical concentrations of biologically active ions at the rate needed for bone cell proliferation and differentiation.

## ***Acknowledgement***

This work was supported by ANR in the National Program of Nanosciences and Nanotechnologies PNANO2005 (project "BIOVERRES" n° ANR-05-NANO-040).

## ***References***

- 
- 1 L. L. Hench, *Journal of Materials Science-Materials in Medicine*, 2006, **17**, 967-978.
  - 2 L. L. Hench, *Journal of Biomedical Materials Research*, 1998, **41**, 511-518.
  - 3 L. L. Hench and J. Wilson, in *Introduction to bioceramics*, ed. L. L. Hench and J. Wilson, World Scientific, 1993.
  - 4 P. Saravanapavan, J. R. Jones, R. S. Pryce and L. L. Hench, *Journal of Biomedical Materials Research Part A*, 2003, **66A**, 110-119.
  - 5 K. Ohura, T. Nakamura, T. Yamamuro, T. Kokubo, Y. Ebisawa, Y. Kotoura and M. Oka, *Journal of Biomedical Materials Research*, 1991, **25**, 357-365.
  - 6 J. P. Zhong and D. C. Greenspan, *Journal of Biomedical Materials Research*, 2000, **53**, 694-701.
  - 7 T. Kokubo, H. M. Kim and M. Kawashita, *Biomaterials*, 2003, **24**, 2161-2175.
  - 8 L. L. Hench, *Biomaterials*, 1998, **19**, 1419-1423.
  - 9 P. Sepulveda, J. R. Jones and L. L. Hench, *Journal of Biomedical Materials Research*, 2001, **58**, 734-740.
  - 10 M. Vallet-Regi, A. J. Salinas and D. Arcos, *Journal of Materials Science-Materials in Medicine*, 2006, **17**, 1011-1017.
  - 11 M. Vallet-Regi, C. V. Ragel and A. J. Salinas, *European Journal of Inorganic Chemistry*, 2003, 1029-1042.
  - 12 P. Sepulveda, J. R. Jones and L. L. Hench, *Journal of Biomedical Materials Research*, 2002, **59**, 340-348.
  - 13 E. Verne, S. Di Nunzio, M. Bosetti, P. Appendino, C. V. Brovarone, G. Maina and M. Cannas, *Biomaterials*, 2005, **26**, 5111-5119.

- 
- 14 P. Saravanapavan, M. H. Patel and L. L. Hench, in *Bioceramics 15*, 2003, pp. 245-248.
- 15 N. Masuda, M. Kawashita and T. Kokubo, *Journal of Biomedical Materials Research Part B-Applied Biomaterials*, 2007, **83B**, 114-120.
- 16 E. Jallot, *Applied Surface Science*, 2003, **211**, 89-95.
- 17 J. M. Nedelec, L. Courtheoux, E. Jallot, C. Kinowski, J. Lao, P. Laquerriere, C. Mansuy, G. Renaudin and S. Turrell, *Journal of Sol-Gel Science and Technology*, 2008, 46, 259-271
- 18 J. Lao, E. Jallot, J.M. Nedelec, *Chem. Mater.*, 2008, *in press*, DOI : cm-2008-00993s
- 19 A. Oki, B. Parveen, S. Hossain, S. Adeniji and H. Donahue, *Journal of Biomedical Materials Research Part A*, 2004, **69A**, 216-221.
- 20 D. B. Jaroch and D. C. Clupper, *Journal of Biomedical Materials Research Part A*, 2007, **82A**, 575-588.
- 21 J. Lao, J. M. Nedelec, Ph. Moretto and E. Jallot, *Surface and Interface Analysis*, 2008, 40, 162-166.
- 22 Linati, L.; Lusvardi, G.; Malavasi, G.; Menabue, L.; Menziani, M. C.; Mustarelli, P.; Segre, U., Qualitative and Quantitative Structure-Property Relationships Analysis of Multicomponent Potential Bioglasses. *J. Phys. Chem. B* 2005, 109, (11), 4989-4998
- 23 Dorozhkin, S. V.; Epple, M., Biological and Medical Significance of Calcium Phosphates. *Angew. Chem. Int. Ed.* **2002**, 41, 3130-3146
- 24 A. Balamurugan, G. Balossier, S. Kannan, J. Michel, A. H. S. Rebelo and J. M. F. Ferreira, *Acta Biomaterialia*, 2007, **3**, 255-262.

Table 1. Experimental composition determined by ICP-AES and specific surface area of the SiO<sub>2</sub>-CaO-ZnO glasses.

<b>Sample</b>	<b>wt.% SiO<sub>2</sub></b>	<b>wt.% CaO</b>	<b>wt.% ZnO</b>	<b>Surface area</b>
Undoped	74.7	25.3	0	26 m <sup>2</sup> g <sup>-1</sup>
Zn1	73.7	25.3	1.0	62 m <sup>2</sup> g <sup>-1</sup>
Zn5	74.0	21.2	4.8	55 m <sup>2</sup> g <sup>-1</sup>

Table 2. Experimental composition at the periphery of SiO<sub>2</sub>-CaO- ZnO glasses obtained by PIXE-RBS after three days of interaction in biological medium. Each concentration value corresponds to the mean of concentrations calculated for several zones of interest. These regions of interest were defined over various samples in order to be ensured of measurements reproducibility.

<b>Sample</b>	<b>% Si</b>	<b>% Ca</b>	<b>% Zn</b>	<b>% P</b>
Undoped	42.3	3.8	0	0
Zn1	33.3	6.3	0	2.7
Zn5	19.7	24.5	0	5.5

## ***Figure Legends***

Figure 1. Elemental maps of SiO<sub>2</sub>-CaO-5%ZnO (Zn5) glass particle before immersion in biological fluid.

Figure 2. SEM image of SiO<sub>2</sub>-CaO bioactive glasses doped with 1% (a) or 5% (b) ZnO.

Figure 3. Elemental maps of SiO<sub>2</sub>-CaO-1%ZnO (Zn1) glass particle after one day of interaction with the biological fluid.

Figure 4. Elemental maps of SiO<sub>2</sub>-CaO-5%ZnO (Zn5) glass particle after one day of interaction with the biological fluid.

Figure 5. Elemental maps of SiO<sub>2</sub>-CaO-5%ZnO (Zn5) glass particle after three days of interaction with the biological fluid.

Figure 6. Ca (squares), Si (triangles), P (circles) and Zn (cross) concentrations in DMEM after interaction with bioactive glasses. Undoped sample is in grey line, Zn1 in dotted lines and Zn5 in straight lines.

Figure 7. Evolution of the Ca/P atomic ratio at the periphery of the glasses during the interaction with biological fluids. Undoped sample is in grey line, Zn1 in dotted line and Zn5 in straight line.

## Figures

Black-and-white figures (to be published)

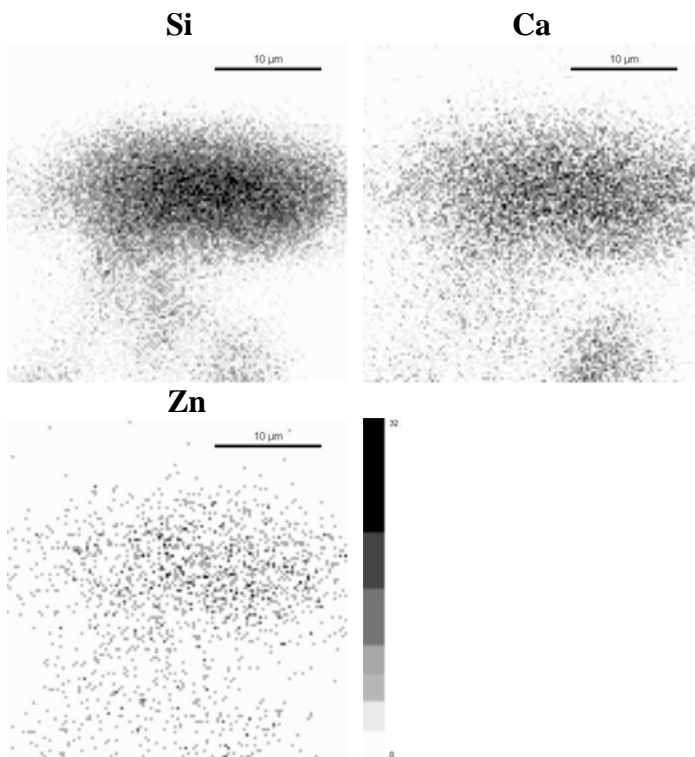


Figure 1. Elemental maps of  $\text{SiO}_2\text{-CaO-5\%ZnO}$  (Zn5) glass particle before immersion in the biological fluid.

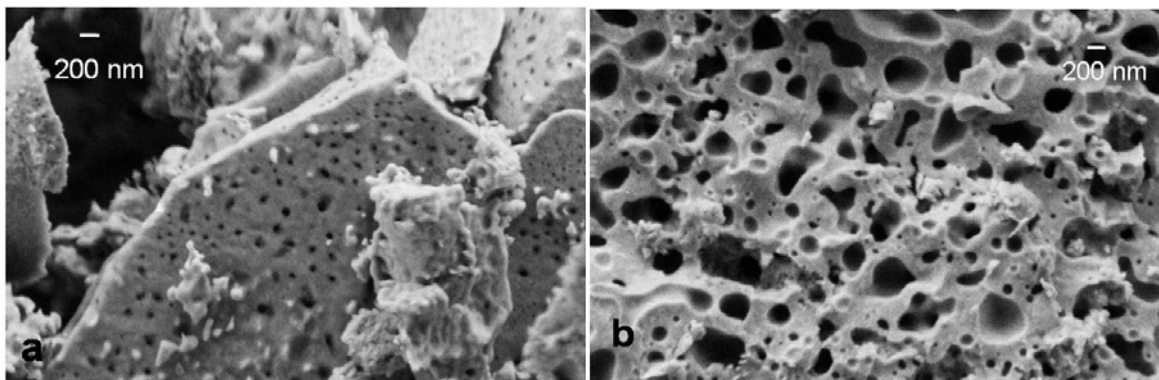


Figure 2. SEM image of  $\text{SiO}_2\text{-CaO}$  bioactive glasses doped with 1% (a) or 5% (b) ZnO.

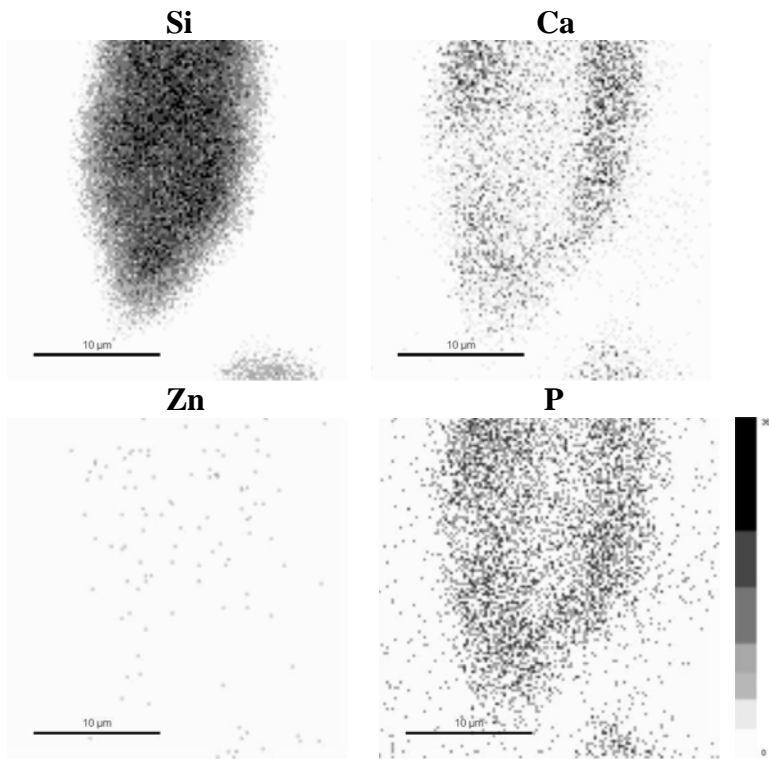


Figure 3. Elemental maps of a  $\text{SiO}_2\text{-CaO-1\%ZnO}$  (Zn1) glass particle after one day of interaction with the biological fluid.

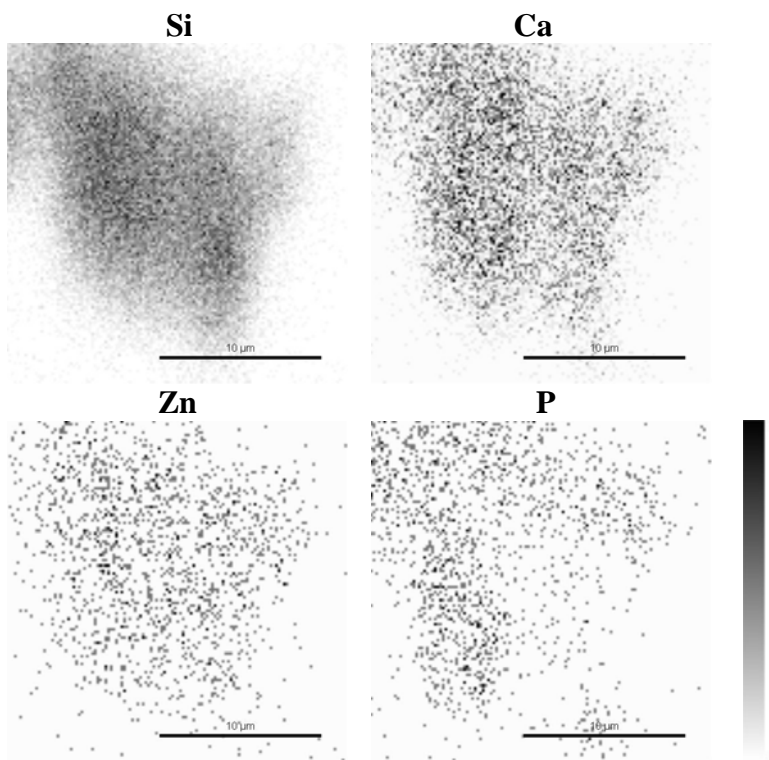


Figure 4. Elemental maps of a  $\text{SiO}_2\text{-CaO-5\%ZnO}$  (Zn5) glass particle after one day of interaction with the biological fluid.



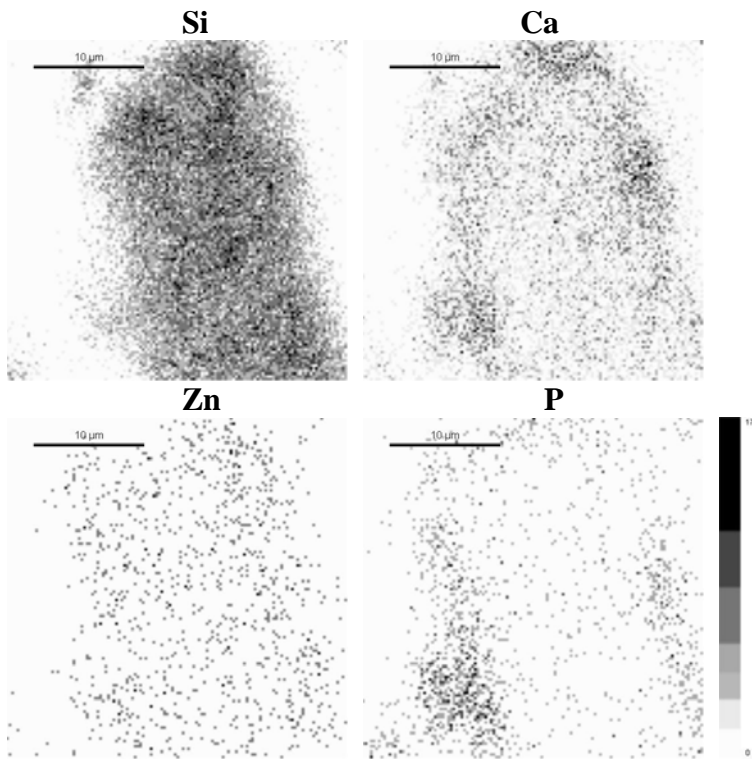


Figure 5. Elemental maps of a  $\text{SiO}_2\text{-CaO-5\%ZnO}$  (Zn5) glass particle after three days of interaction with the biological fluid.

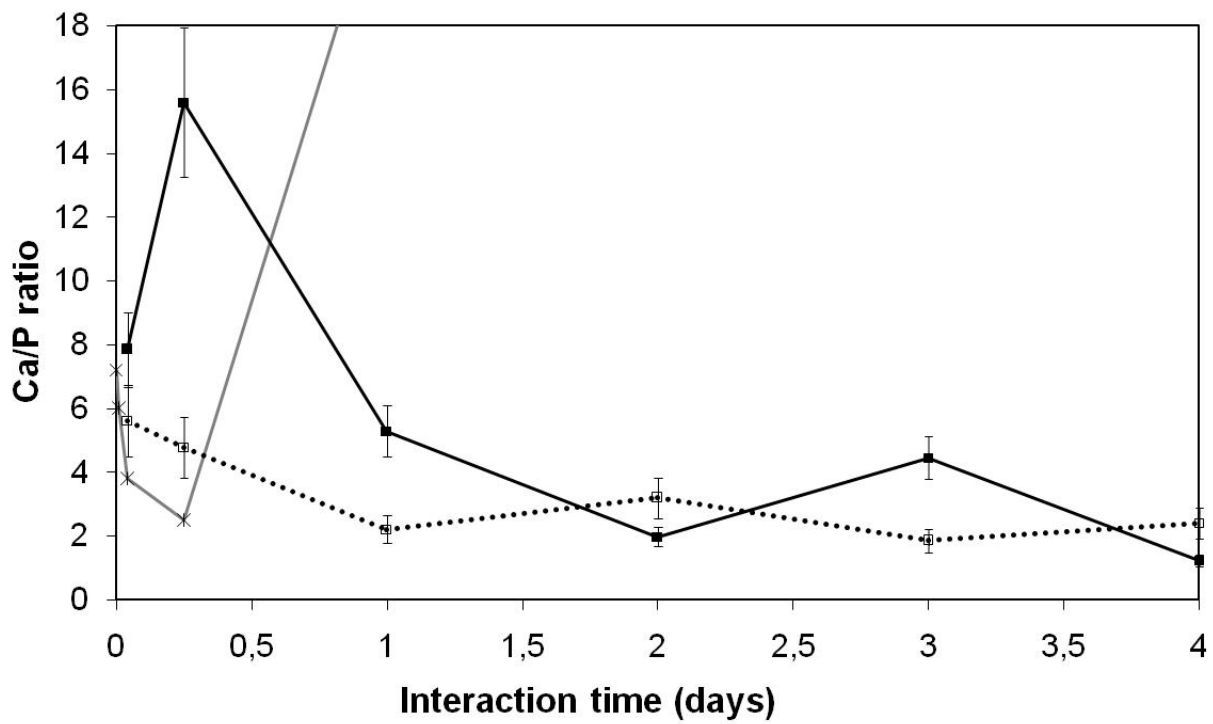


Figure 6. Evolution of the Ca/P atomic ratio at the periphery of the glasses during the interaction with biological fluids. Undoped sample is in grey line, Zn1 in dotted line and Zn5 in straight line.

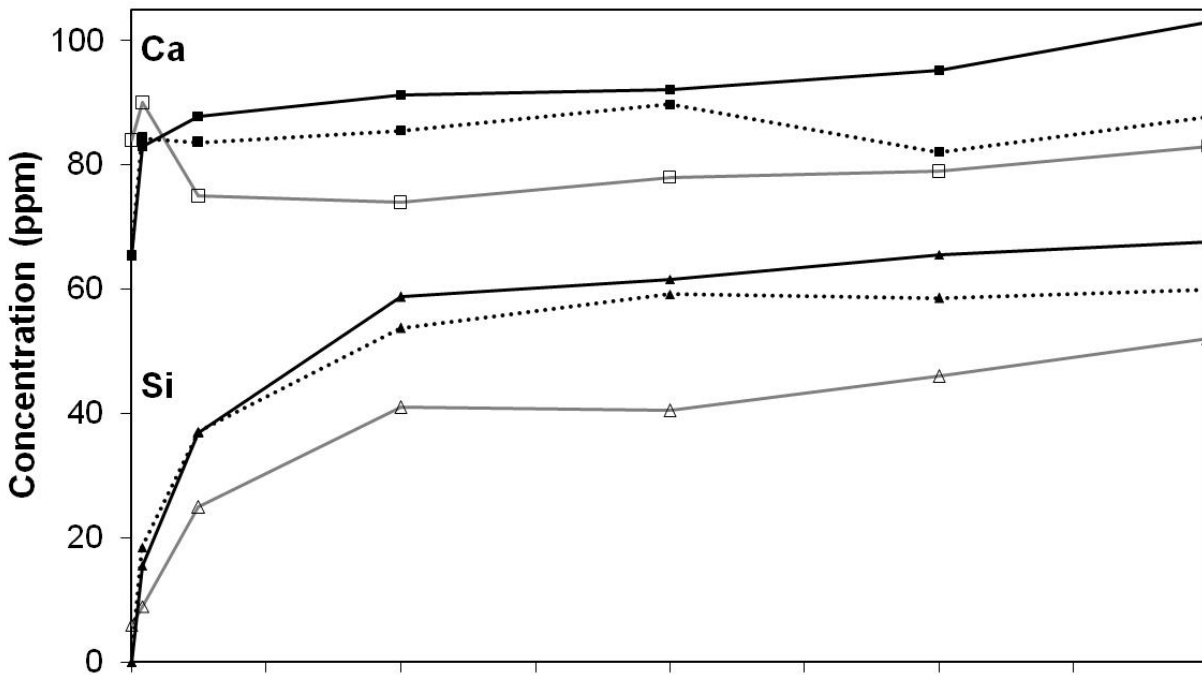
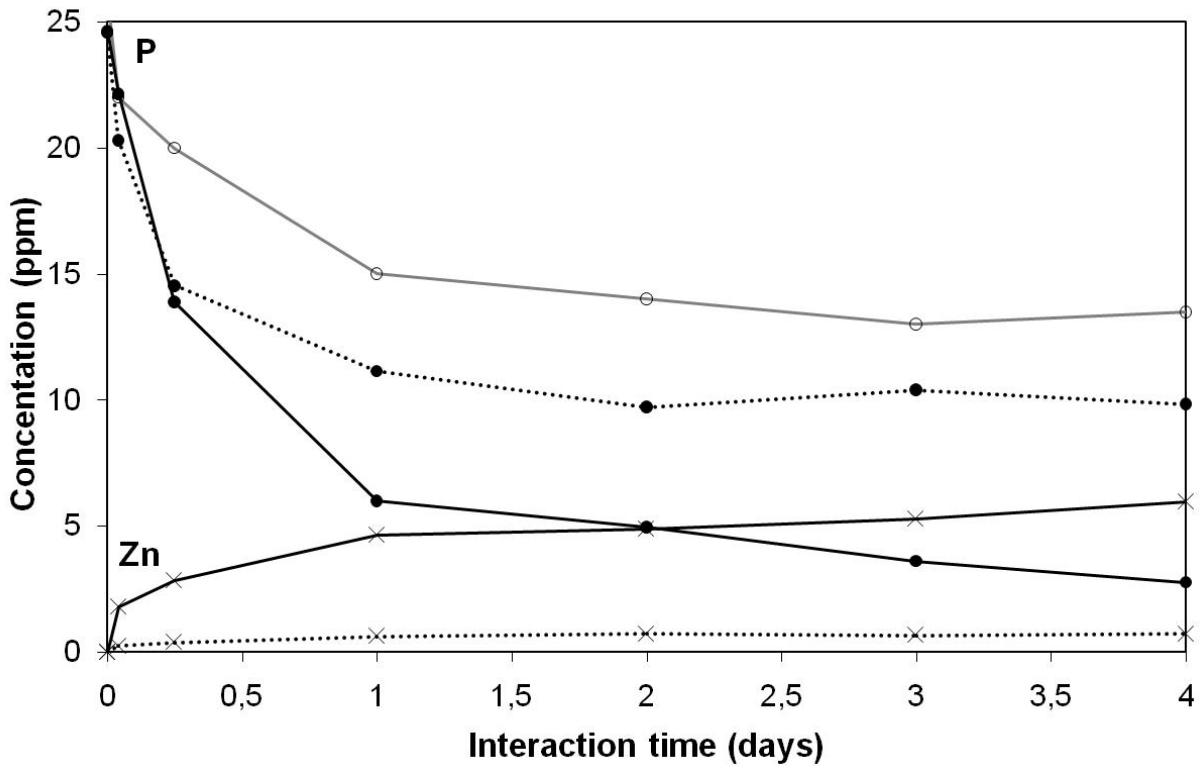


Figure 7. Ca (squares), Si (triangles), P (circles) and Zn (cross) concentrations in DMEM after interaction with bioactive glasses. Undoped sample is in grey line, Zn1 in dotted lines and Zn5 in straight lines.

*Color figures (for the web)*

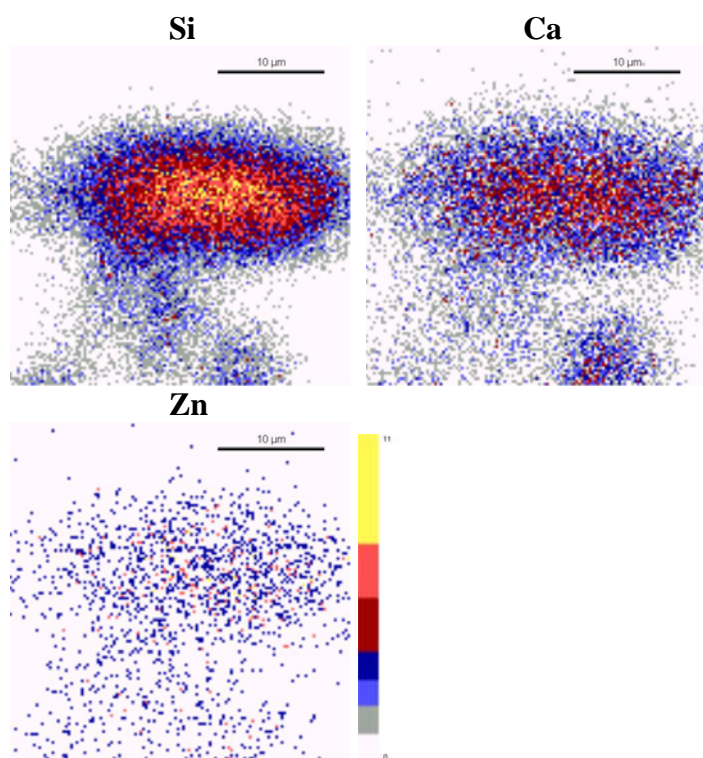


Figure1. Elemental maps of SiO<sub>2</sub>-CaO-5%ZnO (Zn5) glass particles before immersion in biological fluids.

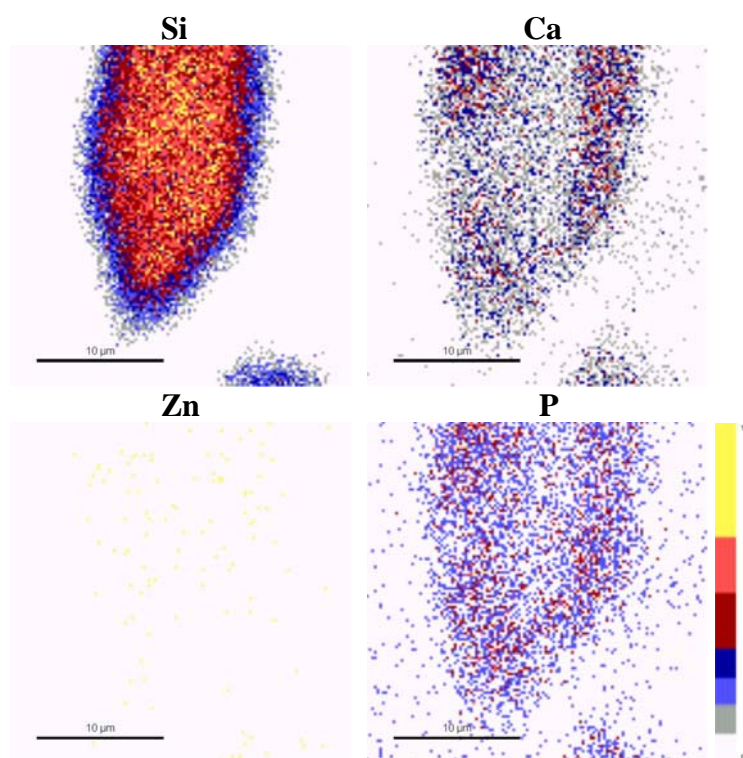


Figure3. Elemental maps of a SiO<sub>2</sub>-CaO-1%ZnO (Zn1) glass particle after one day of interaction with biological fluids.

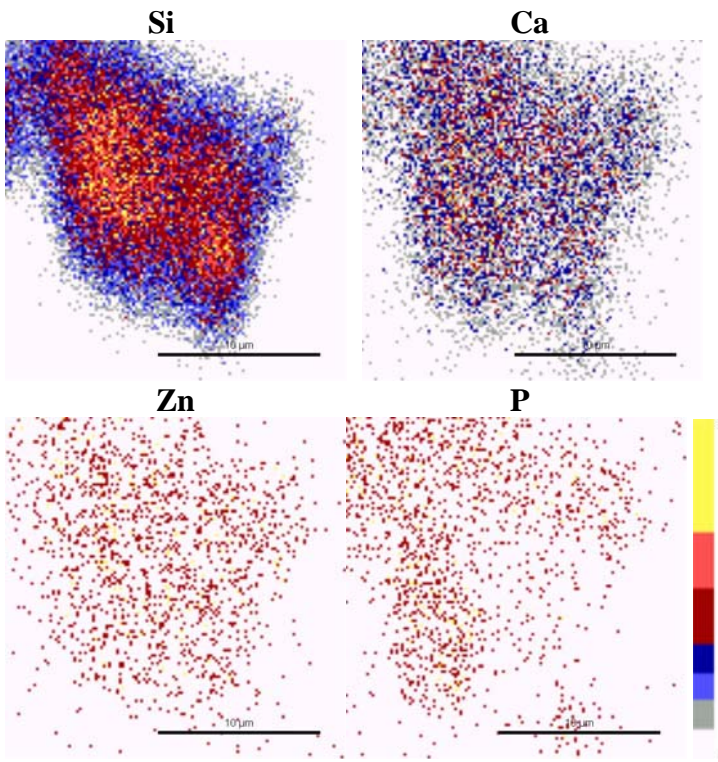


Figure 4. Elemental maps of a  $\text{SiO}_2\text{-CaO-5\%ZnO}$  (Zn5) glass particle after one day of interaction with biological fluids.

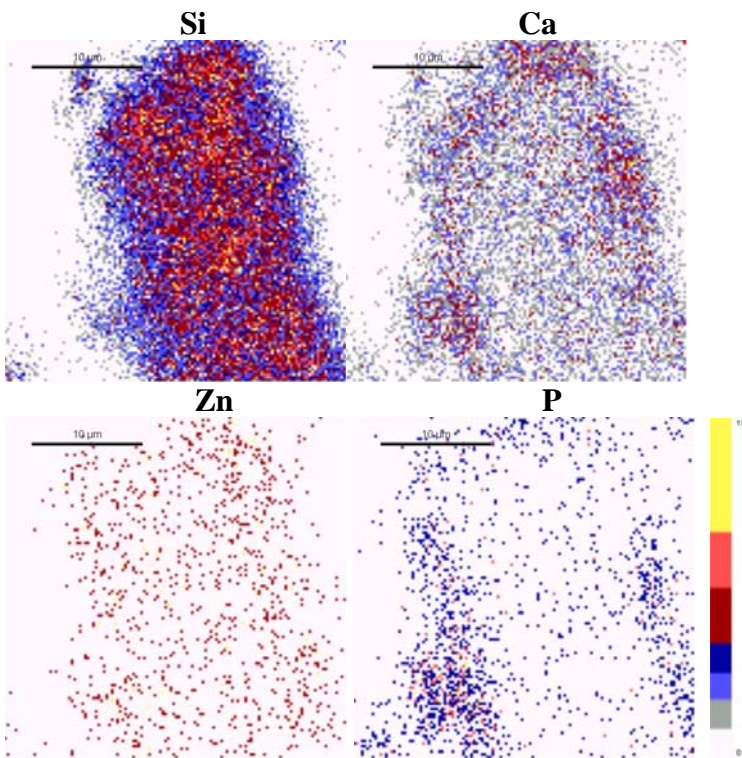


Figure 5. Elemental maps of a  $\text{SiO}_2\text{-CaO-5\%ZnO}$  (Zn5) glass particle after three days of interaction with biological fluids.